Nuclear Science and Techniques (2024) 35:191
https://doi.org/10.1007/s41365-024-01536-9

XPZLIB: an HDF5-format multi-group cross-section library

Bin Fu[1] · Le-Rui Zhang[2] · Ding She[1] · Chun-Lin Wei[1] · Alain Hébert[3]

Received: 26 December 2023 / Revised: 3 May 2024 / Accepted: 8 May 2024 / Published online: 10 October 2024

Abstract
A multi-group cross-section library is fundamental for deterministic lattice physics calculations. Most existing multi-group cross-section libraries are customized for particular computer codes, as well as for particular types of nuclear reactors. This paper presents an HDF5-format multi-group cross-section library named XPZLIB. XPZLIB was produced using a self-developed XPZR module integrated into the NJOY2016 code, and an in-house PyNjoy2022 system was developed for auto-processing. XPZLIB contains detailed data content and well-organized data structures that are user- and developer-friendly. Three typical XPZLIBs with different numbers of energy groups, nuclides, and depletion reaction types were released via the Tsinghua cloud website. Furthermore, the applicability of the released XPZLIBs was investigated using HTGR and PWR lattice calculations, which can provide guidance for applying XPZLIB under different scenarios.

Keywords XPZLIB · Multi-group library · HDF5 format · HTGR · PWR

1 Introduction

A multi-group cross-section library provides fundamental nuclear data for deterministic reactor physics calculations, for example neutron reaction cross-sections and fission-related data. The quality of the multi-group cross-section library can directly influence the accuracy of the lattice physics calculations, and further influence the core physics analysis results. The multi-group cross-section library is processed from evaluated nuclear data libraries, including ENDF/B [1], JEFF [2], JENDL [3], BROND [4], and CENDL [5–7]. The most widely used nuclear data processing program is the NJOY code [8] developed by the Los Alamos National Laboratory (LANL). NJOY can convert the evaluated nuclear data in ENDF-6 [9] format into pointwise or groupwise cross-section libraries.

Most existing multi-group cross-section libraries are customized for particular computer codes, as well as for particular types of nuclear reactors. For example, the widely used WIMS-D library published by the IAEA (https://www-nds.iaea.org/wimsd/). Contains a limited number of nuclides and cross-sectional types, which restricts its application in pressurized water reactor (PWR) analysis [10, 11]. The VSOP code library [12] for high-temperature gas-cooled reactor (HTGR) has a limited number of resonance isotopes. DRAGON5 uses a more delicate data format, DRAGLIB, processed by the PyNjoy2012 system [13–16]. Conventional multi-group libraries are typically stored in complicated data structures that are unfriendly for users and developers.

In this paper, an HDF5-format multi-group cross-section library named XPZLIB is introduced. XPZLIB [17] was previously used by the XPZ-PANGU code [18, 19] in HTGR lattice physics analysis and was well validated in the physical designs of HTR-10 [20, 21], HTR-PM [22, 23], and HTR-PM600 [24]. Recently, it has been improved and extended to light water reactors (LWRs). The new XPZLIB contains comprehensive data adapted to various reactors and a well-organized data structure that is user-friendly. This

This work is supported by the National Key R&D Program of China (2020YFE0202500).

✉ Ding She
sheding@tsinghua.edu.cn

Le-Rui Zhang
zlr17@tsinghua.org.cn

[1] Institute of Nuclear and New Energy Technology, Key Laboratory of Advanced Reactor Engineering and Safety of the Ministry of Education, Tsinghua University, Beijing 100084, China

[2] National Key Laboratory of Nuclear Reactor Technology, Nuclear Power Institute of China, Chengdu 610041, China

[3] Polytechnique Montréal, Montréal, Canada

study aimed to publish the technical details of XPZLIB and make it openly available to the community.

The remainder of this paper is organized as follows. Section 2 introduces the methodologies and tools developed for processing XPZLIB. Section 3 presents the detailed data and structure of XPZLIB. In Sect. 4, the applicability of the three released XPZLIBs for PWR and HTGR lattice calculations is explored. Finally, concluding remarks are presented in Sect. 5.

2 Methods and materials

2.1 XPZLIB processing flow

The XPZLIB processing flow is shown in Fig. 1. The incident neutron data and thermal neutron scattering sublibraries are processed using the built-in modules in NJOY2016 [8], including MODER, RECONR, BROADR, UNRESR, THERMR, and GROUPR. The modules are used for format conversion, resonance reconstruction, Doppler broadening, unresolved cross-section computation, thermalization, and multi-group cross-section generation. The GROUPR output data are in GENDF format. The XPZR module was developed and integrated into NJOY2016 to process GENDF-format data into HDF5-format data in XPZLIB. In addition,

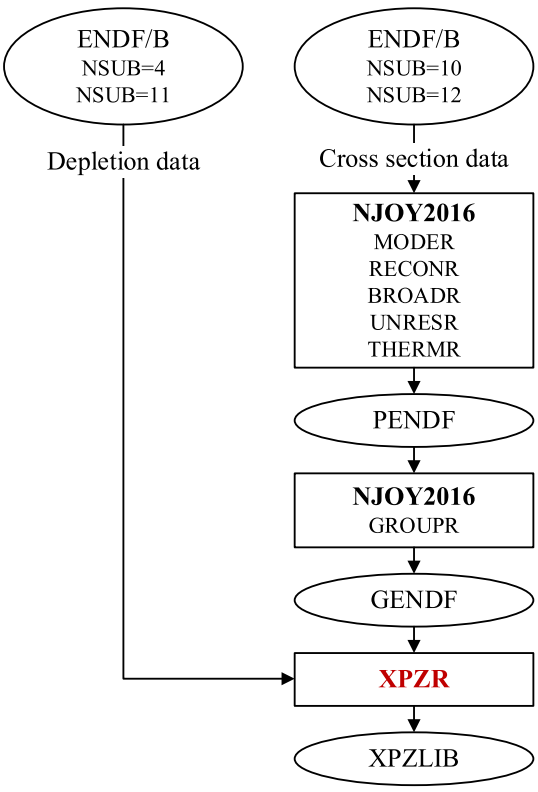

Fig. 1 XPZLIB generation flow

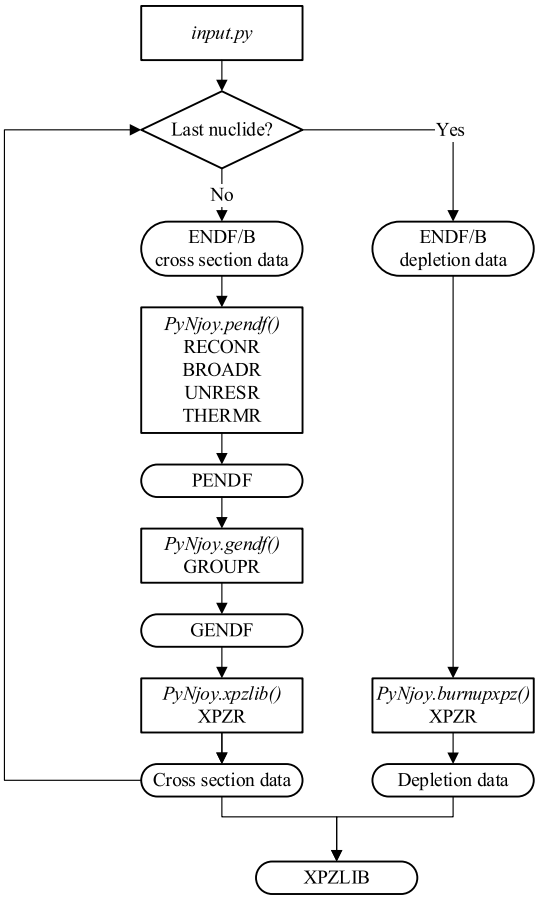

Fig. 2 Workflow of the automated processing system PyNjoy2022

radioactive decay and neutron-induced fission product yield data are processed using XPZR.

2.2 Cross-section and burnup data processing

The related fission data absent from the GENDF file, including the fission spectrum χ and neutron production cross-section $\nu\sigma_f$, are computed as follows:

$$\chi_{g_2} = \frac{\sum_{g_1} \sigma_{f,g_1\to g_2}\phi_{g_1} + \chi_{d,g_2}\sum_{g_1}\nu_{d,g_1}\sigma_{f,g_1}\phi_{g_1}}{\sum_{g_2}\sum_{g_1}\sigma_{f,g_1\to g_2}\phi_{g_1} + \sum_{g_1}\nu_{d,g_1}\sigma_{f,g_1}\phi_{g_1}}, \tag{1}$$

$$\nu_{g_1}\sigma_{f,g_1} = \sum_{g_2}\sigma_{f,g_1\to g_2} + \nu_{d,g_1}\sigma_{f,g_1}, \tag{2}$$

where χ_{g_2}: fission spectrum. χ_{d,g_2}: Delayed neutron fission spectra. ν_{g_1}: Number of neutrons released per fission event. ν_{d,g_1}: Number of delayed neutrons released per fission event. σ_{f,g_1}: Fission cross-section. $\sigma_{f,g_1\to g_2}$: Prompt neutron fission

matrix. ϕ_{g_1}: Weighting flux. g_1: Incident neutron energy group. g_2: Outgoing neutron energy group.

The delayed neutron fission spectrum and the number of delayed neutrons released per fission event can be expressed as

$$\alpha_i = \sum_{g_2} \chi_{i,g_2}^{\mathrm{d},GENDF}, \tag{3}$$

$$\chi_{i,g_2}^{\mathrm{d}} = \frac{\chi_{i,g_2}^{\mathrm{d},GENDF}}{\alpha_i}, \tag{4}$$

$$\nu_{i,g_1}^{\mathrm{d}} \sigma_{\mathrm{f},g_1} = \alpha_i \nu_{g_1}^{\mathrm{d}} \sigma_{\mathrm{f},g_1}, \tag{5}$$

where $\chi_{i,g_2}^{\mathrm{d},GENDF}$: Delayed neutron fission spectrum of the i^{th} group in GENDF. α_i: Fraction of the i^{th} group delayed neutron yield, note that $\alpha_i = \upsilon_i^{\mathrm{d}}/\upsilon^{\mathrm{d}}$. $\chi_{i,g_2}^{\mathrm{d}}$: Delayed neutron fission spectrum of the i^{th} group in XPZLIB. ν_{i,g_1}^{d}: Number of i^{th} group delayed neutrons released per fission event. $\nu_{g_1}^{\mathrm{d}}$: Number of delayed neutrons released per fission event.

In addition to fission-related data, scattering-related data are processed using XPZR. The original elastic scattering cross section in the GENDF file is obtained by assuming that the scattering kernel is in the static state. Thermal scattering models are required to consider the thermal motion of a scattering kernel [25, 26]. Generally, there are two thermal scattering models. One is the free gas model for free atoms, and the other is the S(α, β) model for bounded atoms, e.g., hydrogen nucleus in the water [27]. In the thermal energy region, the total and elastic scattering cross sections are modified by XPZR as follows:

$$\sigma_{\mathrm{thermal\_total}} = \sigma_{\mathrm{total}} - \sigma_{\mathrm{elastic}} + \sigma_{\mathrm{thermal\_scattering}} \tag{6}$$

$$\sigma_{\mathrm{thermal\_elastic}} = \sigma_{\mathrm{thermal\_scattering}} \tag{7}$$

where $\sigma_{\mathrm{thermal\_total}}$: Total cross section in the thermal energy region. $\sigma_{\mathrm{thermal\_elastic}}$: Elastic scattering cross section in the thermal energy region. σ_{total}: Total cross section in the GENDF file. $\sigma_{\mathrm{elastic}}$: Elastic scattering cross section in the GENDF file. $\sigma_{\mathrm{thermal\_scattering}}$: Thermal scattering cross section.

Accordingly, the scattering matrix is modified as follows:

$$\begin{aligned}\sigma_{s,g_1\to g_2} = {} & \sigma_{\mathrm{diffusion},g_1\to g_2} + \sigma_{n2n,g_1\to g_2} \\ & + \sigma_{n3n,g_1\to g_2} + \sigma_{n4n,g_1\to g_2}\end{aligned} \tag{8}$$

Table 1 Data contents of the typical XPZLIB and comparisons with other libraries

	WIMS-D library	VSOP library	Typical XPZLIB
Evaluated nuclear data library	ENDF/B-VII.1, ENDF/B-VI.8	ENDF/B-IV, ENDF/B-V, JEFF-I	ENDF/B-VIII.0
Number of nuclides	185	178	668
Number of nuclides with cross section data	185	178	366
Number of resonance nuclides	28	4	116
Number of nuclides with fission spectrum	^{235}U only	^{235}U and ^{233}U	All fissionable nuclides
Number of nuclides with fission product yields	^{232}Th, ^{233}U, ^{235}U, ^{238}U, ^{239}Pu, ^{240}Pu, ^{241}Pu, ^{242}Pu	^{233}U, ^{235}U, ^{239}Pu, ^{241}Pu	31
Number of nuclides with delayed neutron data	0	0	31
Energy range	10^{-5} eV ~ 10 MeV	10^{-5} eV ~ 10 MeV	10^{-4} eV ~ 20 MeV
Range of resonance energy	4 eV ~ 9.118 keV	not clear	4 eV ~ 320.65 keV
Number of energy groups	69/172	98	SHEM-361 [28]
Cross sections and quantities dependent on temperature	(n, abs), (n, f)	(n, abs), (n, f)	(n, tot), (n, f), (n, γ), (n, p), (n, α), (n, n), (n, 2n), (n, 3n), (n, 4n), (n, n'), (n, np), (n, d), (n, t), (n, 2α), $\sigma_{s,g1\to g2}$, $\nu\sigma_{\mathrm{f}}$, χ, $\nu_{\mathrm{d},1\text{-}6}\sigma_{\mathrm{f}}$, $\chi_{\mathrm{d},1\text{-}6}$
Cross sections dependent on background cross section	(n, abs), (n, f)	(n, abs), (n, f)	(n, tot), (n, f), (n, γ), (n, n), $\sigma_{s,g1\to g2}$, $\nu\sigma_{\mathrm{f}}$, $\nu_{\mathrm{d},1\text{-}6}\sigma_{\mathrm{f}}$
Isotopes with S (α, β) data	^{1}H_H_2O, ^{2}H_D_2O, ^{1}H_ZrH	0	^{1}H_H_2O, ^{2}H_D_2O, ^{1}H_CH_2, ^{1}H_ZrH, ^{9}Be, ^{12}C_Graphite, ^{90}Zr_ZrH
Depletion reaction channels	(n, 2n), (n, f), (n, γ)	(n, 2n), (n, 3n), (n, f), (n, γ), (n, p), (n, α)	Decay, (n, 2n), (n, 3n), (n, 4n), (n, f), (n, np), (n, γ), (n, p), (n, d), (n, t), (n, α), (n, 2α)

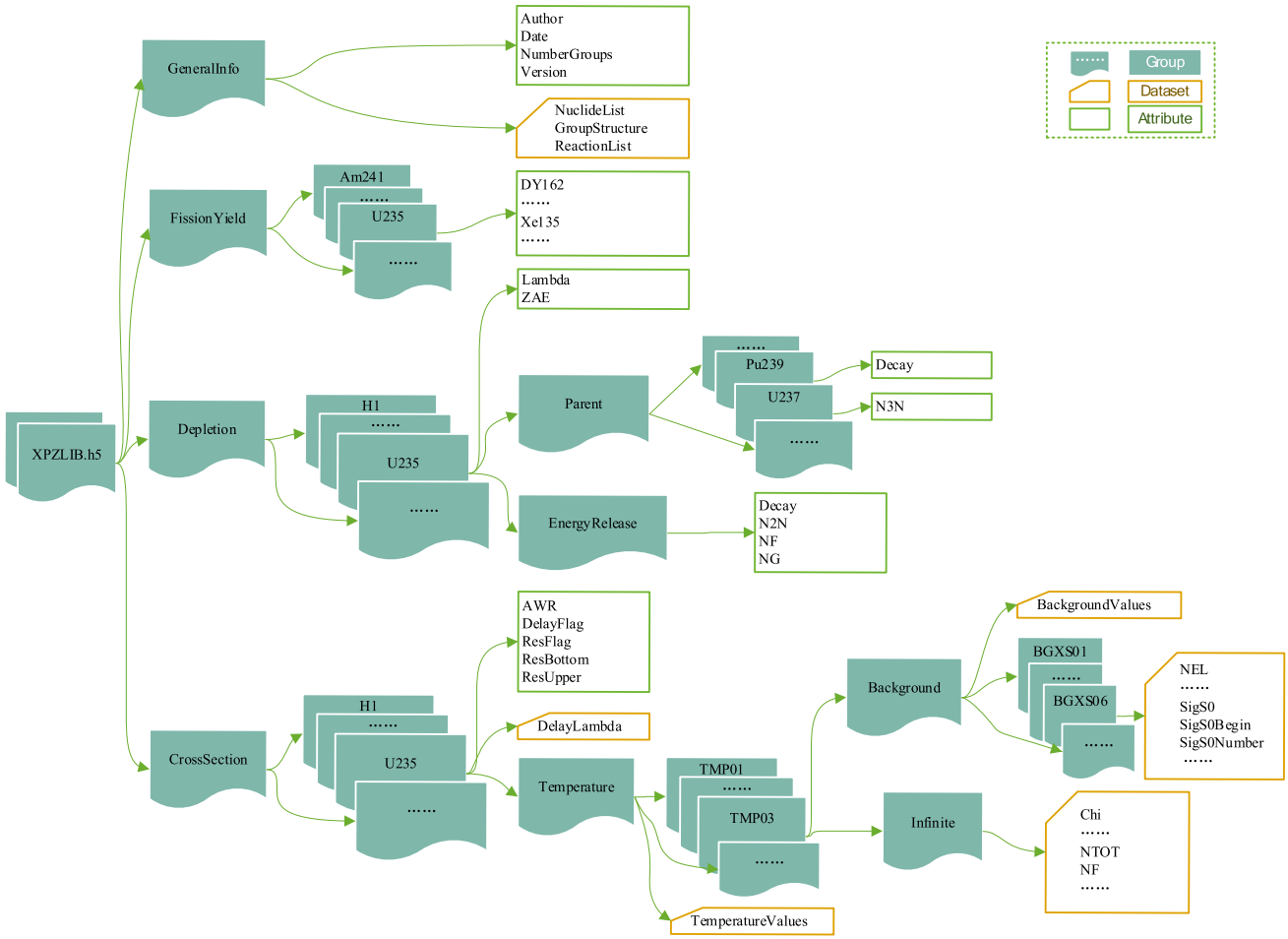

Fig. 3 (Color online) XPZLIB structure

Fig. 4 Sketch map of the **GeneralInfo** group

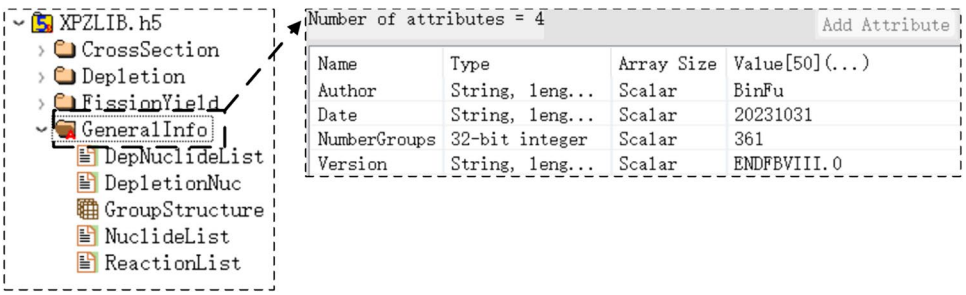

where $\sigma_{\text{diffusion},g_1\to g_2}$: Diffusion matrix consisting of elastic and inelastic scattering matrices. This is equivalent to the thermal scattering matrix in the thermal energy region. $\sigma_{n2n,g_1\to g_2}$: (n, 2n) matrix. $\sigma_{n3n,g_1\to g_2}$: (n, 3n) matrix. $\sigma_{n4n,g_1\to g_2}$: (n, 4n) matrix.

In addition to cross-sectional data processing, XPZR can read radioactive decay and fission product yield data from the corresponding ENDF/B sublibraries and generate a compressed burnup chain. Nuclides with short half-lives and small fission yields, which are negligible for neutron transport calculations, can be grouped according to user-defined criteria. The typical criteria used in XPZR are a nuclide half-life of less than 30 days and a fission yield of less than 0.01%. XPZR can also accept a user-defined nuclide list and depletion channels, leading to different levels of detailed burn-up chains.

Table 2 Structure and description of the **GeneralInfo** group

Content	Description
GeneralInfo	
Date	processing date
Version	the version of evaluated nuclear data library used
Author	processing author
NumberGroups	number of energy groups
GroupStructure	energy group bins
NuclideList	list of nuclides with cross section data
DepNuclideList	list of nuclides with burnup-related data
ReactionList	list of depletion reactions

Bold: Group; *Italic*: Attribute; Normal font: Dataset

2.3 Automated processing system

A complete XPZLIB contains hundreds of nuclides, each with a corresponding NJOY input card and output file. To generate the input cards and manage the output files automatically, an automated processing system, PyNjoy2022, was developed based on the PyNjoy2012 system [15]. Figure 2 shows the workflow of the PyNjoy2022 system.

PyNjoy2022 contains an important Python script named **PyNjoy.py**, which provides the following functions: PyNjoy.pendf(): Processes the evaluated data in ENDF-6 format into pointwise cross-sectional data in PENDF format. PyNjoy.gendf(): Processes PENDF into group-wise cross-sectional data in GENDF format; PyNjoy.xpzlib(): Processes GENDF into XPZLIB data format via XPZR; PyNjoy.burnupxpz(): Generates depletion and fission yield data via XPZR.

The **Input.py** script contains a general XZPLIB description, for example, its weighting flux and energy group structure. It also contains the processing parameters of all the nuclides that must be included in XPZLIB. For each nuclide, **Input.py** calls the functions in **PyNjoy.py** to complete the data processing. First, PyNjoy.pendf() and PyNjoy.gendf() are used to generate PENDF and GENDF, respectively. Then, PyNjoy.xpzlib() is called to generate the cross-sectional data block of the current nuclide, which is automatically appended to the HDF5-format XPZLIB. After all nuclides have been processed, PyNjoy.burnupxpz() is called to generate the depletion data and add them to XPZLIB.

3 Data content and data structure of XPZLIB

XPZLIB provides important neutron reaction cross-section data and other quantities at given temperatures. The influence of dilution on the resonant nuclides was considered. S(α, β) data is included in XPZLIB for moderator isotopes, such as ^{12}C in graphite, ^{1}H in water, among others. XPZLIB also provides depletion data, including the branch ratio and recoverable energy of the depletion reactions. In

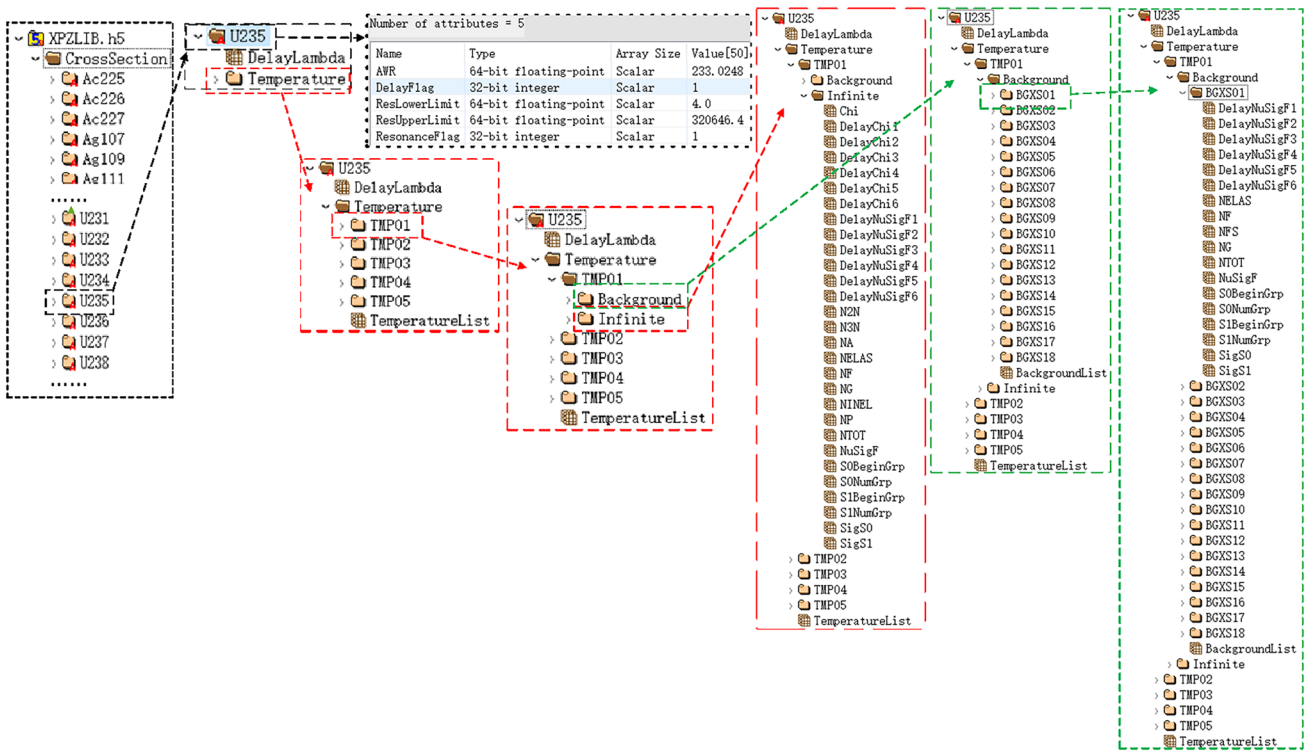

Fig. 5 Sketch map of the **CrossSection** group

Table 3 Structure and description of the **Cross section** group

Content	Description
Cross section	
H1	nuclide name
…	
U235	
…	
AWR	ratio of the isotope's atom mass to the neutron mass
DelayFlag	flag indicating whether the nuclide includes delayed data
ResFlag	flag indicating whether the nuclide includes resonance data
ResLowerLimit	resonance energy bottom /eV
ResUpperLimit	resonance energy upper /eV
DelayLambda	delayed neuron precursor's decay constant
Temperature	temperature-dependent data
Temperature List	list of temperature values
TMP01	data at the first temperature
…	
TMP03	
…	
Background	dilution-dependent data
BackgroundList	list of background values
BG01	XS and parameters dataset at a certain temperature at a certain dilution
…	
BG10	
…	
XS and quantities	
Infinite	XS and parameters dataset at a certain temperature at infinite dilution
XS and quantities	

addition, the fission-product yields are available for important nuclides. The above data can be easily utilized in general lattice physics computations involving resonance, transport, and depletion.

Considering the characteristics of various reactors, XPZLIB can be processed using different parameters such as the number of nuclides, energy group structure, temperature grid points, background cross sections, and depletion reaction types. Table 1 compares the data contents of WIMS-D, VSOP, and XPZLIB.

XPZLIB is generated in HDF5 file format [29], which stores data according to groups, datasets, and attributes. It is convenient for developers to access HDF5 files using interfaces such as HighFive [30]. Figure 3 shows the overall XPZLIB data structure. Four top-level groups are used to store general information, cross-sectional data, depletion data, and fission yield data.

The **GeneralInfo** group records the basic library information. A sketch map of **GeneralInfo** is shown in Fig. 4, and a detailed description is provided in Table 2.

The **CrossSection** group mainly stores the temperature- and dilution-dependent neutron cross sections of all reactions of the listed nuclides. The data are stored in a three-loop structure comprising nuclide, temperature, and dilution loops. A sketch map of **CrossSection** is shown in Fig. 5, and Table 3 presents its data structure and corresponding descriptions.

In the temperature loop, the neutron cross sections at a certain temperature are stored in a group named **TMP##**. For resonance nuclides, the neutron cross sections are dependent on the dilution or background cross sections. Moreover, a dilution loop is observed in the **TMP##** group. The **BGXS##** group contains resonance cross sections at a certain dilution. For non-resonant nuclides, only infinite-dilution cross sections are provided in the **Infinite** group. In addition to the cross-sectional data, other quantities are also provided. Table 4 lists all the cross sections and other quantities used in XPZLIB.

The scattering matrix is stored in MATXS format [31]. As presented in Table 5, for target group g, **BeginGrp** indicates the index of the highest incident energy group g' for which the scattering cross section to group g is present, and **NumGrp** indicates the total number of incident groups for which the scattering cross sections of group g are present. The corresponding scattering cross sections are stored in the **SigS** dataset. XPZLIB can include

Table 4 Cross sections and quantities keywords used in XPZLIB

Data	Keywords in XPZLIB	Burnup reaction
Neutron spectrum	Chi	
(n, tot)	NTOT	
(n, n)	NELAS	
(n, n')	NINEL	
(n, 2n)	N2N	✓
(n, 3n)	N3N	✓
(n, f)	NF	✓
(n, np)	NNP	✓
(n,4n)	N4N	✓
(n, γ)	NG	✓
(n, p)	NP	✓
(n, d)	ND	✓
(n, t)	NT	✓
(n, α)	NA	✓
(n, 2α)	N2A	✓
Decay	Decay	
Scattering matrix of 0 and 1st order	SigS0; SigS1	
Scattering beginning group	S0BeginGrp; S1BeginGrp	
Number of scattering groups	S0NumGrp; S1NumGrp	
NuSigmaF	NuSigF	
Delayed NusigmaF	DelayNuSigF	
Delayed neutron spectrum	DelayChi1 ~ DelayChi6	
Neutron flux spectrum	NFS	

Table 5 The format of scattering matrix in XPZLIB

Group index G	**BeginGrp**	**NumGrp**	**SigS** (Scattering matrix)
g	g'	n	g' → g g'-1 → g ... g'-n + 1 → g

higher-order scattering cross-section data, although only P_0 and P_1 scattering cross sections are used in transport calculations.

To save data storage, the dilution-dependent cross-sectional data are stored as follows. Under infinite dilution, the data are stored for all energy groups. However, under finite dilution, only the data for the resonance-energy groups are present, which are stored as the incremental resonance integral relative to that under infinite dilution:

$$\delta\sigma_{x,g,\sigma_0} = \sigma_{x,g,\sigma_0} * \varphi_{g,\sigma_0} - \sigma_{x,g,\sigma_{\text{infinite}}} \tag{9}$$

where σ_{x,g,σ_0} is the resonance cross section of group g for reaction x at dilution σ_0; $\sigma_{x,g,\sigma_{\text{infinite}}}$ is the resonance cross section at infinite dilution; and φ_{g,σ_0} is the averaged fine spectrum function at dilution σ_0, which is related to the **NFS** data as

$$NFS_g = \varphi_{g,\sigma_0} - \varphi_{g,\sigma_{\text{infinite}}} \tag{10}$$

It is noted that $\varphi_{g,\sigma_{\text{infinite}}} = 1$.

The **FissionYield** group has a set of sublevel groups named fissirious nuclides, where all fission products and their yields are stored, as shown in Fig. 6 and described in Table 6.

The **Depletion** group is used to construct the burn-up chain. The branch ratio $R_{i,j,x}$ is the proportion of reaction x of parent nuclide i that leads to the production of child nuclide j. This information is stored in the **Parent** group for each child nuclide in the burn-up chain. In addition, the **EnergyRelease** group records the recoverable energy of each nuclide for all burnup channels. Detailed information regarding the **Depletion** group is provided in Fig. 7 and Table 7.

4 Validation

4.1 Released XPZLIBs

In general, a multi-group library with more detailed data is expected to have better accuracy and wider applicability, but at the expense of increased computational cost. Thus, it is important to use a sufficiently accurate XPZLIB for certain applications. As shown in Table 8, three typical XPZLIBs were processed with different numbers of energy groups, nuclides, and depletion reaction types to meet different user requirements. The three XPZLIBs were released via the Tsinghua cloud website (https://cloud.tsinghua.edu.cn/d/a7c675735ad8497f8a87).

4.2 Test cases

Table 9 lists the numerical cases based on HTGR and PWR fuel elements. For HTGR, two cases were taken from the standard fuel pebbles of HTR-10 [20] and HTR-PM [22]. The fuel pebble's structure is shown in Fig. 8. It consists of a fuel region filled with dispersed TRISO particles [32] and a graphite shell. The TRISO particles consist of a spherical fuel kernel of UO_2 with multi-layer coatings, including a low-density pyrolytic carbon (PyC) buffer layer, inner high-density PyC layer, silicon carbide (SiC) layer, and outer high-density PyC layer. The detailed parameters of the two fuel pebbles and coated particles are listed in Table 10.

For the PWR, two cases were constructed using a typical PWR assembly pin and an MOX fuel pin [33]. Because the XPZ code is limited to treating one-dimensional (1D)

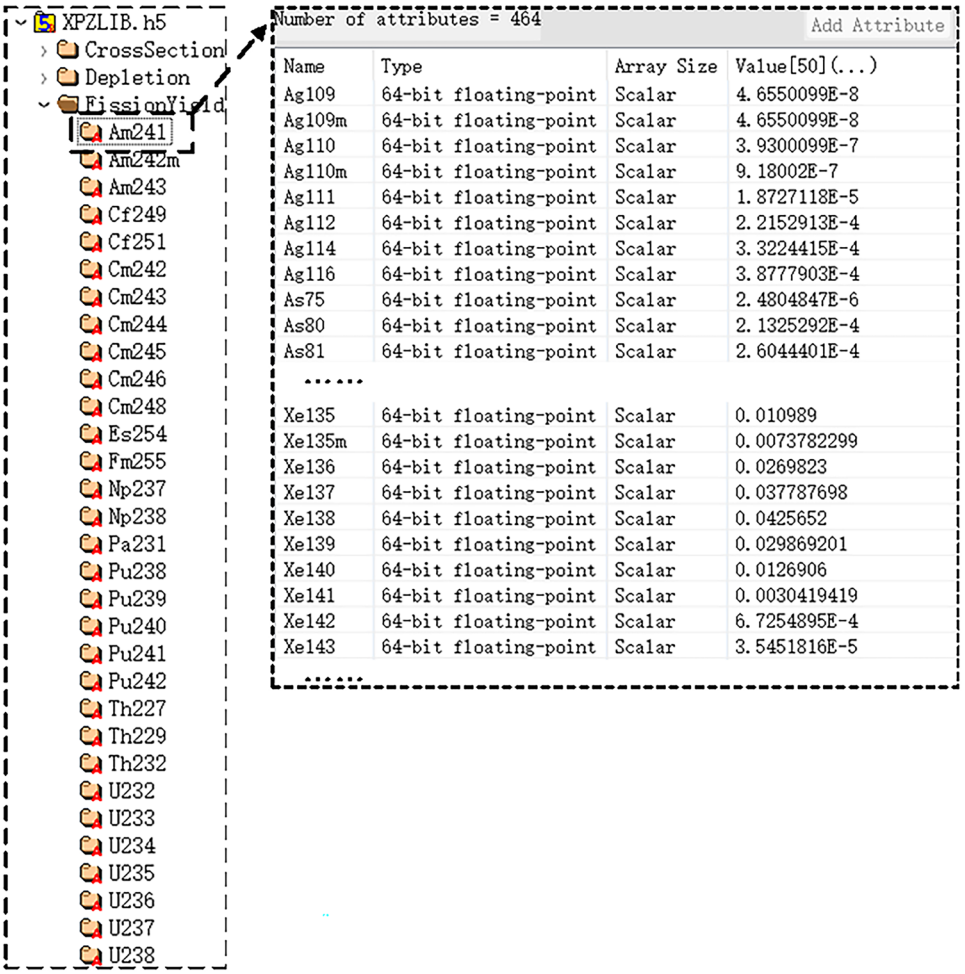

Fig. 6 Sketch map of the **FissionYield** group

Table 6 Structure and description of the **Fission Yield** group

Content	Description
Fission Yield	fission products and their yields
Pa231	
…	
U235	
…	
Ag109	fission yield of Ag109
…	
Zr96	fission yield of Zr96

geometries, the square-lattice model was converted to a volumetric-equivalent cylinder model, as illustrated in Fig. 9. The key parameters are specified in Table 11.

4.3 Numerical results

The three released XPZLIBs were used in the XPZ code to simulate the HTGR and PWR cases. The XPZ code is used in lattice physics computations for 1D models, and is also used for decay heat estimation. XPZ uses the subgroup method with intermediate resonance approximation to treat the resonance effect [34–36]. The OpenMC Monte Carlo (MC) code [37], which uses a continuous energy cross-section library processed from the ENDF/B VIII.0 nuclear data, was used to provide the reference results. In the MC

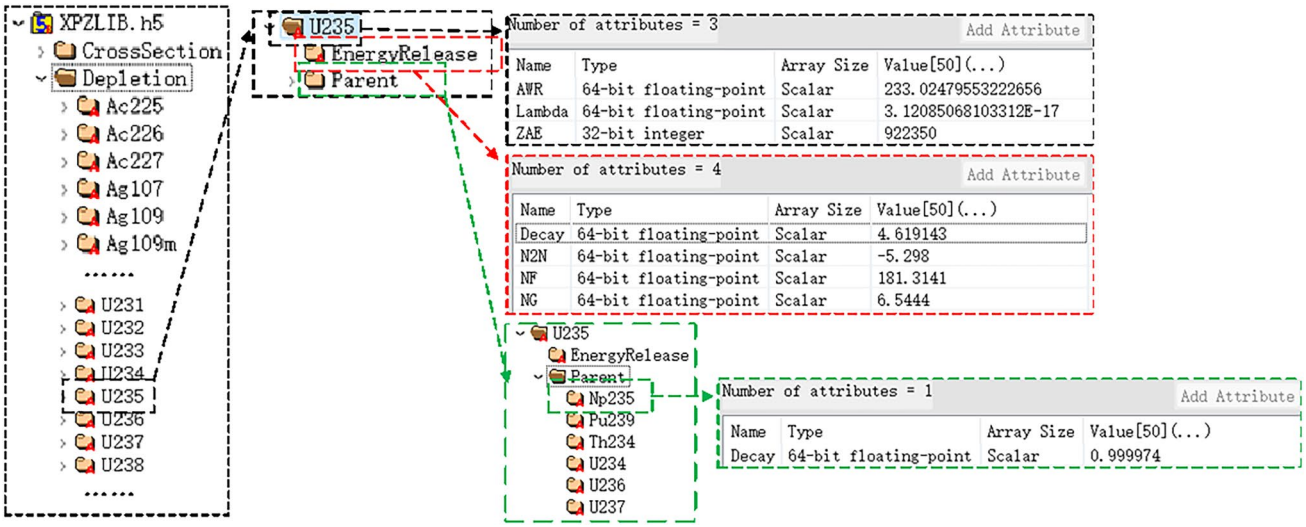

Fig. 7 Sketch map of the Depletion group

Table 7 Structure and description of the **Depletion** group

Content	Description
Depletion	transmutation data
H1	
…	
U235	
…	
Lambda	decay constant
ZAE	ZAE = $Z\times10{,}000 + A\times10 + E$; Z is the number of atomics; A is the mass number and E is the energy state of the isotope (0 denotes the ground state; 1, 2 and 3 denotes the 1st, 2nd and 3rd excited state, respectively)
Parent	parent nuclide
Am241	
…	
Pu238	
…	
N4N	the branch ratio of the parent nuclide (Pu238) producing the daughter nuclide (U235) by N4N reaction
…	
Energy release	energy released from a certain reaction
Decay	energy release from nuclide decay /MeV
……	
NG	energy release from (n, γ) reaction /MeV

Table 8 Processing parameters of the released XPZLIBs

	Simplified XPZLIB	Standard XPZLIB	Refined XPZLIB
Energy group structure	WIMS-69	SHEM-361	
Resonance energy range	9.118 keV ~ 4 eV (15 ~ 27 group) for all resonance nuclides	320.65 keV ~ 4 eV (31 ~ 276 group) for important heavy nuclides, e.g., ^{232}Th, ^{235}U, ^{238}U, ^{239}Pu; 18.58 keV ~ 4 eV (52 ~ 276 group) for other resonance nuclides	
Number of nuclides with cross section data for transport calculation	183	322	366
Number of nuclides for depletion calculation	183	322	668
Depletion channels	4 depletion channels: (n, 2n); (n, fission); (n, γ); decay	12 depletion channels: (n, 2n); (n, 3n); (n, 4n); (n, fission); (n, np); (n, γ); (n, p); (n, d); (n, t); (n, α); (n, 2 α); decay	

Table 9 Numerical cases based on HTGR and PWR fuel elements

Reactor	Case
HTGR	1 HTR-10 fuel pebble with 17% ^{235}U enrichment
	2 HTR-PM fuel pebble with 8.5% ^{235}U enrichment
PWR	3 PWR fuel pin with 3% ^{235}U enrichment
	4 PWR fuel pin with Mixed oxide fuel (MOX) material

calculations, the neutron generation parameter was set to 2000, with 200 inactive generations and 10,000 neutrons per generation.

Transport calculations were performed for all test cases. The resulting k_{eff} values and their differences from the OpenMC reference results are presented in Table 12. The k_{eff} standard deviation for the OpenMC calculations was < 20 pcm. It was found that the simplified XPZLIB provided marginally acceptable accuracy for all test cases. This is likely because the WIMS-69 energy group structure cannot account for complex resonance effects; therefore, its application is limited to typical PWRs [38, 39]. The standard and refined XPZLIBs produced identical results and exhibited good accuracy for all test cases. This is due to the use of the SHEM-361 energy group structure and the expanded resonance energy range.

In the burnup calculations of the HTGR cases, a power density of 74.074 W/gU and maximum burnup of 100 MWD/kgU were obtained for the HTR-10 pebble, with values of 97.146 W/gU and 110 MWD/kgU, respectively, for the HTR-PM pebble. In the burnup calculations of the PWR cases, a power density of 40.45 W/gU and a maximum burnup of 60 MWD/KgU was employed.

The k_{eff} dependence on burnup for the four cases is shown in Fig. 10, respectively. The k_{eff} standard deviation of the OpenMC reference calculations was < 40 pcm. For all test cases, the k_{eff} results obtained using the standard and refined XPZLIBs agreed well with the Monte Carlo reference result, with a maximum difference below 200 pcm. However, the simplified XPZLIB can provide acceptable accuracy only in the typical PWR fuel pin case, whereas it yields up to 1000 pcm errors in the HTGR cases. This is mainly due to the difference in the neutron spectra of the HTR and PWR cases. A simplified XPZLIB with a WIMS-69 energy structure was optimized based on the PWR neutron spectrum. The HTR cases require a more refined energy structure.

To compare the applicability of the XPZLIBs in nuclide transmutation simulations, important nuclides from the HTR-10 fuel pebble at the final burnup step were analyzed. Table 13 lists the atomic densities and relative errors of the standard and simplified XPZLIBs compared with those of the refined XPZLIB. The standard XPZLIB provided

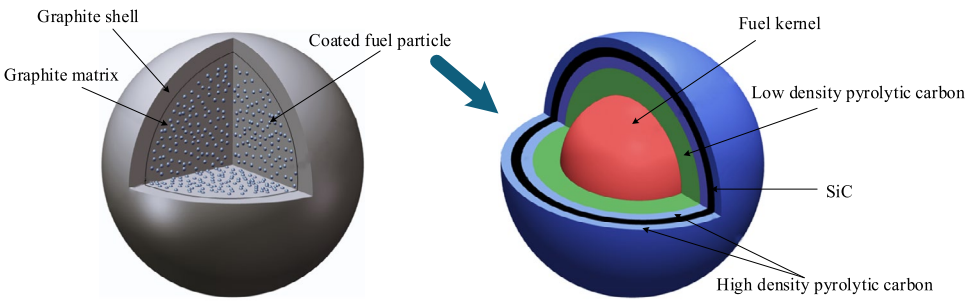

Fig. 8 HTGR fuel pebble model

Table 10 Parameters of the HTGR fuel pebble element

Physical parameter	HTR-10	HTR-PM
Fuel pebble		
Uranium weight in single fuel pebble	5 g	7 g
Enrichment of ^{235}U (weight)	17%	8.5%
Diameter of the fuel pebble	6 cm	6 cm
Diameter of the fuel zone in the fuel pebble	5 cm	5 cm
Density of graphite (including matrix and outer shell)	1.73 g/cm^3	1.74 g/cm^3
Impurities represented by EBC in uranium	4 ppm	0.5 ppm
Impurities represented by EBC in graphite	1.3 ppm	0.795 ppm
Coated fuel particle		
Radius of the kernel	250 μm	250 μm
Thickness of low density PyC	90 μm	95 μm
Thickness of inner high density PyC	40 μm	40 μm
Thickness of SiC	35 μm	35 μm
Thickness of outer high density PyC	40 μm	40 μm
Density of UO_2	10.4 g/cm^3	10.4 g/cm^3
Density of low density PyC	10.4 g/cm^3	1.05 g/cm^3
Density of high density PyC	1.9 g/cm^3	1.9 g/cm^3
Density of SiC	3.18 g/cm^3	3.18 g/cm^3

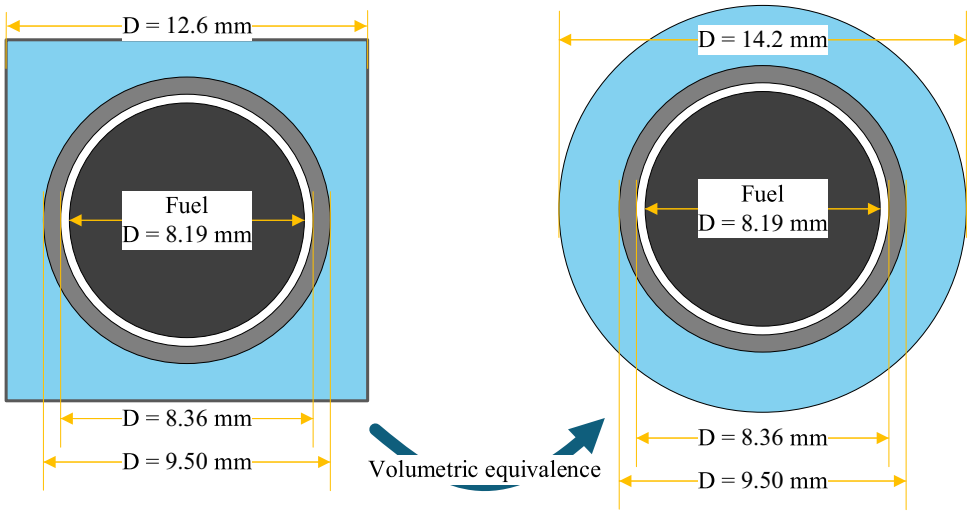

Fig. 9 (Color online) PWR pin cell model

consistent results for most of the important nuclides compared to the refined library. Conversely, the simplified XPZLIB model exhibited considerable errors for some important nuclides. For instance, ^{137}Cs, an important isotope for burn-up measurements [40], presented a discrepancy of approximately 4%.

Decay heat calculations are crucial for nuclear reactor safety analysis. It is known that decay heat accounts for approximately 6% of the operational power at the moment of reactor shutdown. It decreases rapidly within several hours owing to the decay of short half-life nuclides; thereafter, it is dominated by the decay of middle and long half-life nuclides. For accurate decay heat simulations, it is necessary to consider short half-life nuclides; however, they are usually neglected in neutron transport calculations.

To test the applicability of the XPZLIBs for decay heat calculations, the HTR-10 fuel pebble was depleted to 100 MWD/kgU with a designed power density of 74.074 W/gU, followed by a cooling time of five days. The reference results were obtained using a superfine XPZLIB with an uncompressed burn-up chain containing 3821 nuclides and 12 depletion channels, which are comparable to the delicate libraries adopted by nuclide inventory calculation codes such as NUIT [41] and ORIGEN-S [42]. As shown in Fig. 11, the results obtained from the refined XPZLIB are in excellent agreement with the reference results, demonstrating its

Table 11 PWR fuel pin parameters

Case		3	4
Type of PWR fuel pin		Typical PWR fuel pin	PWR fuel pin with MOX fuel
Density of the fuel (g/cm^3)		10.4	10.4
Density of atom in the fuel (g/cm^3)	^{235}U	0.2750	0.0665
	^{238}U	8.8925	8.918
	^{238}Pu	0	0.0050
	^{239}Pu	0	0.0936
	^{240}Pu	0	0.0444
	^{241}Pu	0	0.1440
	^{242}Pu	0	0.0235
	^{241}Am	0	0.0035
	^{16}O	1.2324	1.2335
Density of the water (g/cm^3)		0.7	0.7
Boron in water (ppm)		500	500

applicability in decay heat calculations. Both the standard and simplified XPZLIBs exhibited significant deviations from the reference results after a short shutdown period, as the two libraries lacked many short half-life nuclides.

5 Conclusion

In this paper, an HDF5-format multi-group cross-section library named XPZLIB is introduced. XPZLIB was processed using the open-source NJOY2016 code with a built-in XPZR module and external Python scripts. XPZLIB contains detailed data content and well-organized data structures, making it applicable to various reactors and user- and developer-friendly.

Three typical XPZLIBs with different numbers of energy groups, nuclides, and depletion reaction types were obtained from the Tsinghua cloud website. Their applicability was analyzed in transport, burn-up, and decay heat

Table 12 k_{eff} calculation results obtained using OpenMC and XPZ

Case	XPZ results and differences against OpenMC				
	OpenMC	Simplified XZPLIB	Δk_{eff} (pcm)	Standard XPZLIB Refined XPZLIB	Δk_{eff} (pcm)
HTR-10	1.68237	1.68664	427	1.68224	− 13
HTR-PM	1.56081	1.56686	605	1.56054	− 27
PWR	1.28288	1.27828	− 85	1.28327	39
PWR with MOX fuel	1.09532	1.08854	− 562	1.09668	136

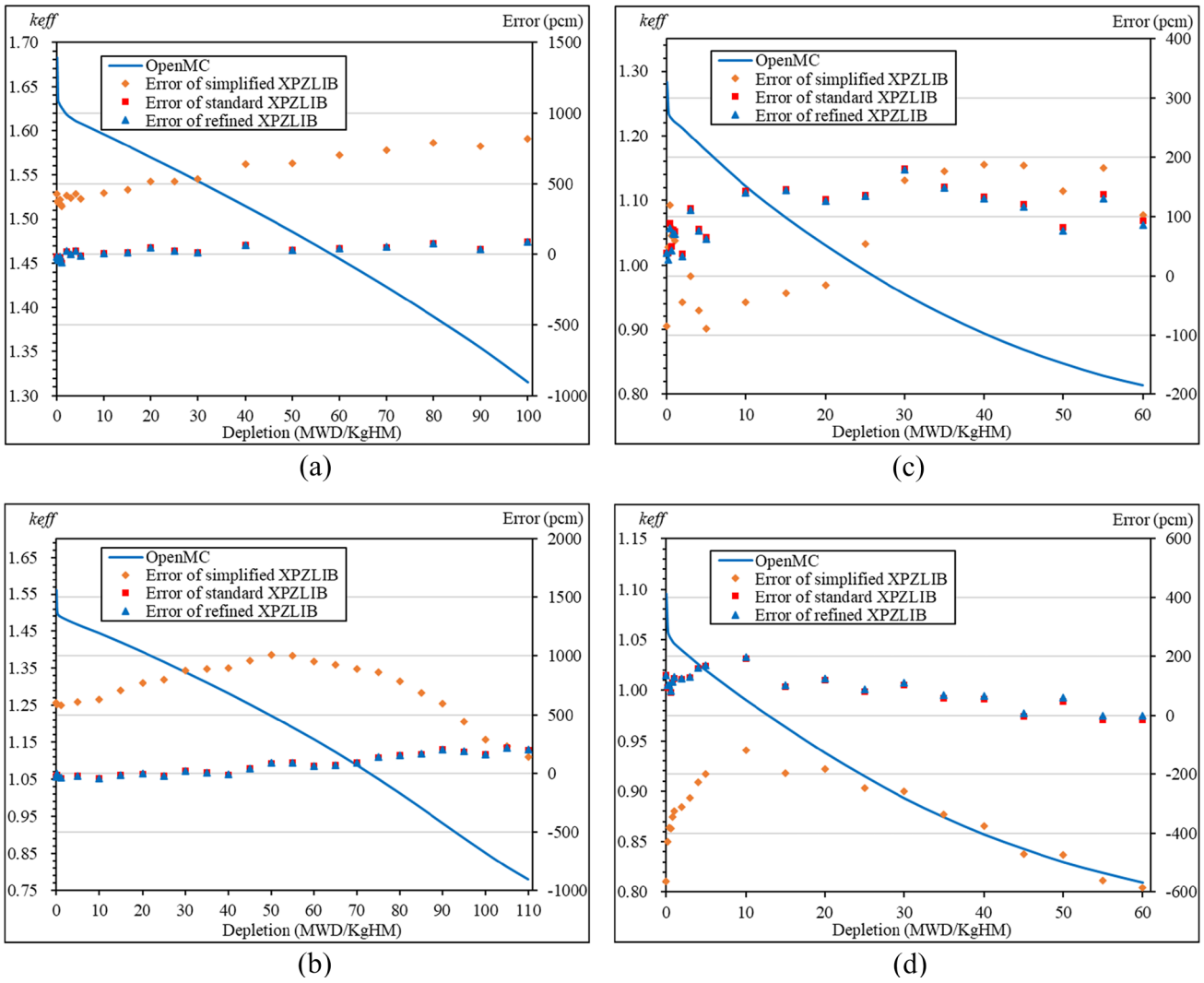

Fig. 10 k_{eff} with burnup for the **a** HTR-10 fuel pebble, **b** HTR-PM fuel pebble, **c** typical PWR fuel pin, and **d** PWR-MOX fuel pin

Table 13 Nuclide composition of the HTR-10 fuel pebble at the final burn-up step

Nuclide name	Atomic density (/barn/cm) calculated with refined XPZLIB	Relative error (%) of standard XPZLIB	Relative error (%) of simplified XPZLIB
Kr85	4.559×10^{-6}	1.25×10^{-2}	–*
Rb85	1.732×10^{-5}	1.73×10^{-2}	26.0
Sr88	7.737×10^{-5}	1.16×10^{-2}	–
Y91	7.331×10^{-6}	3.67×10^{-2}	–
Zr91	1.219×10^{-4}	4.35×10^{-2}	5.86
Mo96	3.198×10^{-6}	1.00×10^{-2}	2.44
Mo97	1.401×10^{-4}	7.21×10^{-2}	–
Ru100	7.866×10^{-6}	4.35×10^{-2}	–
Ag109	2.881×10^{-6}	1.09×10^{-1}	2.83
Te128	9.366×10^{-6}	2.00×10^{-2}	–
I127	4.085×10^{-6}	4.56×10^{-1}	1.18
I129	1.420×10^{-5}	2.61×10^{-2}	–
Xe132	1.153×10^{-4}	1.39×10^{-2}	–
Cs134	7.404×10^{-6}	1.41×10^{-1}	39.7
Cs137	1.400×10^{-4}	0	4.43
Ba134	3.188×10^{-6}	2.41×10^{-1}	–
Ce141	4.459×10^{-6}	1.66×10^{-2}	–
Pr141	1.300×10^{-4}	1.85×10^{-2}	–
Np237	1.662×10^{-5}	6.02×10^{-4}	3.03
Pu238	2.806×10^{-6}	3.56×10^{-4}	1.61
Pu239	1.920×10^{-4}	2.60×10^{-3}	5.18
Pu240	5.305×10^{-5}	1.13×10^{-3}	2.90
Pu241	3.020×10^{-5}	2.32×10^{-3}	3.58
Pu242	7.465×10^{-6}	3.08×10^{-3}	1.56

*The simplified XPZLIB does not include this nuclide

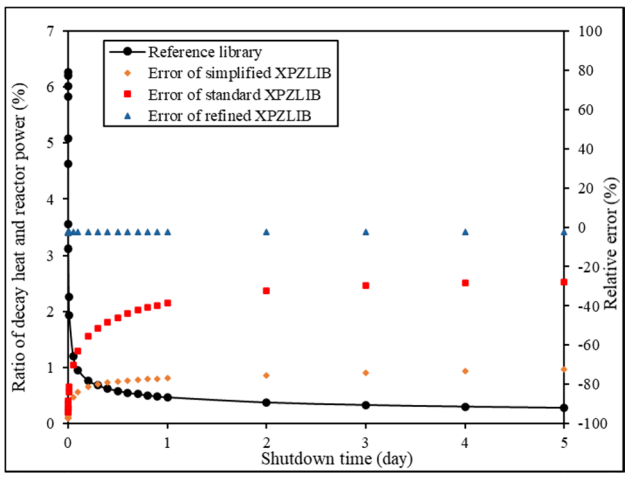

Fig. 11 Decay heat results for the HTR-10 fuel pebble

calculations across HTGRs and PWRs. The transport and burn-up results indicated that the simplified XPZLIB is suitable for typical PWRs. The standard XPZLIB is applicable for both PWRs and HTGRs, and may potentially be applicable to other reactors. This is mainly due to the finer energy group structure and more depletion reaction types used by the standard XPZLIB. The refined XPZLIB incorporates additional short-lived actinides and fission products, which demonstrated excellent accuracy in the decay heat calculations.

Based on these characteristics and actual performance, the standard XPZLIB is recommended for use in most thermal reactors. The simplified XPZLIB provides acceptable accuracy in typical PWRs and is expected to perform similarly to the WIMS-D library. The refined XPZLIB is recommended for detailed decay heat or nuclide transmutation simulations.

Acknowledgements The released XPZLIBs were downloaded from the Tsinghua cloud website (https://cloud.tsinghua.edu.cn/d/a7c675735ad8497f8a87). Readers are encouraged to use them and provide feedback.

Author contributions All authors contributed to the study conception and design. Material preparation, data collection and analysis were performed by Bin Fu, Le-Rui Zhang, Ding She, Chun-Lin Wei and Alain Hébert. The first draft of the manuscript was written by Bin Fu and all authors commented on previous versions of the manuscript. All authors read and approved the final manuscript.

Declarations

Conflict of interest The authors declare that they have no competing interests.

References

1. D.A. Brown, M.B. Chadwick, R. Capote et al., ENDF/B-VIII.0: The 8th major release of the nuclear reaction data library with CIELO-project cross sections, new standards and thermal scattering data. Nucl. Data Sheet **148**, 1–142 (2018). https://doi.org/10.1016/j.nds.2018.02.001
2. A. Koning, R. Forrest, M. Kellett et al., *The JEFF-3.1 Nuclear Data Library, JEFF Report 21*. (The OECD Nuclear Energy Agency, ISBN 92–64–02314–3, 2006). Available: https://www.oecd-nea.org/jcms/pl_36784/the-jeff-3-1-nuclear-data-library.
3. K. Shibata, O. Iwamoto, T. Nakagawa et al., JENDL-4.0: a new library for nuclear science and engineering. J. Nucl. S. Technol. **48**(1), 1–30 (2011). https://doi.org/10.3327/jnst.48.1
4. S. Zabrodskaya, A. Ignatyuk, V. Kosheev et al., ROSFOND-Russian national library of neutron data VANT (Voprosi Atomnoy Nauki i Techniki) ser. Nucl Constents **1**, 3–21 (2007)
5. Z.G. Ge, Z.X. Zhao, H.H. Xia et al., The updated vversion of Chinese evaluated nuclear data library (CENDL-3.1). J. Korean Phys. Soc. **59**, 1052–1056 (2011). https://doi.org/10.3938/jkps.59.1052
6. Z.G. Ge, R.R. Xu, H.C. Wu et al., CENDL-3.2: The new version of Chinese general purpose evaluated nuclear data library. EPJ. Web. Conf. **239**, 09001 (2020). https://doi.org/10.1051/epjconf/202023909001
7. X. Ruan, Nuclear data measurement progress in China. Nucl. Tech. (in Chinese) **46**, 080003 (2023). https://doi.org/10.11889/j.0253-3219.2023.hjs.46.080003

8. D.W. Muir, R.M. Boicourt, A.C. Kahler et al., *The NJOY Nuclear Data Processing System, Version 2016*. (Los Alamos National Laboratory, New Mexico, LA-UR-17–20093, 2016)
9. A. Trkov, M. Herman and D. A. Brown (ed), *ENDF-6 Formats Manual*. (National Nuclear Data Center Brookhaven National Laboratory Upton, New York, 2018). https://doi.org/10.2172/2007538
10. F. Leszczynski, D. López Aldama, A. Trkov, *WIMS-D library update*. (Vienna, Austria: International Atomic Energy Agency; 2007).
11. J.R. Askew, F.J. Fayers, P.B. Kemshell, General description of the lattice code WIMS. J. Brit. Nucl. Ener. Soc. **5**, 564–585 (1966)
12. E. Teuchert, U. Hansen, K. A. Haas et al., V. S. O.P. ('94) Computer Code System for Reactor Physics and Fuel Cycle Simulation. (1994)
13. G. Marleau, A. Hébert, R. Roy, *A user guide for DRAGON version5*. (École Polytechnique de Montréal, Montréal, IGE-335, 2019).
14. A. Hébert, G. Marleau, R. Roy, *A Description of the DRAGON and TRIVAC Version5 Data Structures.* (École Polytechnique de Montréal, Montréal, IGE-351 2019).
15. A. Hébert, *PyNjoy-2012: A system for producing cross-section libraries for the DRAGON lattice code*. ND2016, International Conference on Nuclear Data for Science and Technology, Bruges, Belgium, (2016)
16. D.W. Muir, R.M. Boicourt, A.C. Kahler, et al., *The NJOY Nuclear Data Processing System, Version 2012*. (Los Alamos National Laboratory, New Mexico, LA-UR-12–27079, 2017).
17. Lerui Zhang, Ding She, Lei Shi, Richard Chambon, Alain Hébert, Multi-group cross section library generation for HTGR lattice physics code XPZ. J. Phys. Conf. Ser. **2048**, 012028 (2021). https://doi.org/10.1088/1742-6596/2048/1/012028
18. D. She, Z.H. Liu, L. Shi, XPZ: Development of a lattice code for HTR. Ann. Nucl. Energy **97**, 183–189 (2016). https://doi.org/10.1016/j.anucene.2016.07.017
19. D. She, J. Guo, Z.H. Liu et al., PANGU code for pebble-bed HTGR reactor physics and fuel cycle simulations. Ann. Nucl. Energy **126**, 48–58 (2019). https://doi.org/10.1016/j.anucene.2018.11.005
20. Z.X. Wu, D.C. Lin, D.X. Zhong, The design features of the HTR-10. Nucl. Eng. Des. **218**, 25–32 (2002). https://doi.org/10.1016/S0029-5493(02)00182-6
21. D. She, F.B. Chen, B. Xia et al., Simulation of the HTR-10 operation history with the PANGU code. Front. Energy Res. **9**, 704116 (2021). https://doi.org/10.3389/fenrg.2021.704116
22. Z.Y. Zhang, Z.X. Wu, Y.L. Sun et al., Design aspects of the Chinese modular high-temperature gas-cooled reactor HTR-PM. Nucl. Eng. Des. **236**, 485–490 (2006). https://doi.org/10.1016/j.nucengdes.2005.11.024
23. D. She, B. Xia, J. Guo et al., Prediction calculations for the first criticality of the HTR-PM using the PANGU code. Nucl. Sci. Tech. **32**, 90 (2021). https://doi.org/10.1007/s41365-021-00936-5
24. Z.Y. Zhang, Y.J. Dong, Q. Shi et al., 600-MWe high-temperature gas-cooled reactor nuclear power plant HTR-PM600. Nucl. Sci. Tech. **33**, 101 (2022). https://doi.org/10.1007/s41365-022-01089-9
25. J.U. Koppel, D.H. Houston, *Reference manual for ENDF thermal neutron scattering data*. (U. S. Atomic Energy Commission, San Francisco, GA--8774, 1968). https://doi.org/10.2172/4075168
26. T.J. Zu, Y.Q. Tang, Z.P. Huang et al., Treatments of thermal neutron scattering data and their effect on neutronics calculations. Front. Energy Res. **9**, 779261 (2021). https://doi.org/10.3389/fenrg.2021.779261
27. M. Mattes, J. Keinert, *Thermal Neutron Scattering Data for the Moderator Materials H_2O, D_2O and ZrHx in ENDF-6 Format and as ACE Library for MCNP(X) Codes*. (IAEA, VIENNA, INDC(NDS)-0470, 2005).
28. A. Hébert, *A. Santamarina, Refinement of the Santamarina-Hfaiedh energy mesh between 22.5 eV and 11.4 keV*. International Conference on Reactor Physics, Interlaken, Switzerland, (2008)
29. S. Koranne, *Hierarchical data format 5: HDF5 Handbook of Open Source Tools* (Springer, Boston, 2011), pp.191–200
30. HighFive: An easy-to-use, header-only C++ library for HDF5 (2023), https://bluebrain.github.io/HighFive/poster/.
31. R.E. MacFarlane, *TRANSX 2: A Code for Interfacing MATXS Cross-Section Libraries to Nuclear Transport Codes*. (Los Alamos National Laboratory, New Mexico, LA-12312-MS, 1992).
32. P.A. Demkowicz, B. Liu, J.D. Hunn, Coated particle fuel: Historical perspectives and current progress. J. Nucl. Mater. **515**, 434–450 (2019). https://doi.org/10.1016/j.jnucmat.2018.09.044
33. M.C. Betancourt, C.R.G. Hernández, D.S. Dominguez, L.Y. Mazaira, C.A. Brayner, J.A.R. García, S.M. Iglesias, Mixed-oxide fuel strategies in an integral pressurized water reactor. Prog. Nucl. Energy **139**, 103844 (2021). https://doi.org/10.1016/j.pnucene.2021.103844
34. D.G. Cacuci (ed.), *Handbook of nuclear engineering* (Springer, Karlsruhe, 2010)
35. S.T. Peng, X.F. Jiang, S.H. Zhang et al., Subgroup method with resonance interference factor table. Ann. Nucl. Energy **59**, 176–187 (2013). https://doi.org/10.1016/j.anucene.2013.04.005
36. R. Goldstein, E.R. Cohen, Theory of resonance absorption of neutrons. Nucl. Sci. Eng. **13**, 132–140 (2017). https://doi.org/10.13182/NSE62-1
37. P.K. Romano, N.E. Horelik, B.R. Herman et al., OpenMC: a state-of-the-art Monte Carlo code for research and development. Ann. Nucl. Energy **82**, 90–97 (2015). https://doi.org/10.1016/j.anucene.2014.07.048
38. M.R. Riham, A. Amin Esmat, Neutron multiplication factor calculation for PWR MOX fuel pin cells with WIMS-D5 code. J. Nucl. Part. Phys. **6**, 7 (2016)
39. Z.Y. Dong, J. Wu, X.B. Ma et al., Development and verification of a 281-group WIMS-D library based on ENDF/B-VII.1. Ann. Nucl. Energy **91**, 189–194 (2016). https://doi.org/10.1016/j.anucene.2016.01.014
40. G. Radócz, A. Gerényi, S. Czifrus et al., Determination of 137Cs content in fuel assemblies of a zero power reactor by Monte Carlo based efficiency calibration. Ann. Nucl. Energy **130**, 512–517 (2019). https://doi.org/10.1016/j.anucene.2019.01.010
41. J. Li, D. She, L. Shi et al., The NUIT code for nuclide inventory calculations. Ann. Nucl. Energy **148**, 107690 (2020). https://doi.org/10.1016/j.anucene.2020.107690
42. O. W. Hermann, R. M. Westfall, *ORIGEN-S: SCALE system module to calculate fuel depletion, actinide transmutation, fission product buildup and decay, and associated radiation source terms*. (SCALE6.1 Manual. ORNL/TM-2005/39, Oak Ridge National Laboratory 2011).